Initiation of inflammatory tumorigenesis by CTLA4 insufficiency due to type 2 cytokines

Jason Miska,[1]* Jen Bon Lui,[1]* Kevin H. Toomer,[1] Priyadharshini Devarajan,[1] Xiaodong Cai,[3,6] JeanMarie Houghton,[4] Diana M. Lopez,[1,6] Maria T. Abreu,[5,6] Gaofeng Wang,[2,6] and Zhibin Chen[1,6]

[1]Department of Microbiology and Immunology and [2]Hussman Institute for Human Genomics, University of Miami Miller School of Medicine, Miami, FL
[3]Department of Electrical and Computer Engineering, University of Miami, Coral Gables, FL
[4]Division of Gastroenterology, Department of Medicine, University of Massachusetts Medical School, Worcester, MA
[5]Division of Gastroenterology, Department of Medicine and [6]Sylvester Comprehensive Cancer Center, University of Miami, Miami, FL

Genetically predisposed CTLA4 insufficiency in humans is associated with gastric cancer development, which is paradoxical to the prototypical role of CTLA4 in suppressing antitumor immunity. CTLA4 is a critical immune checkpoint against autoimmune disorders. Autoimmunity has been implicated in protumor or antitumor activities. Here, we show that CTLA4 insufficiency initiates de novo tumorigenesis in the mouse stomach through inflammation triggered by host–intrinsic immune dysregulation rather than microbiota, with age-associated progression to malignancy accompanied by epigenetic dysregulation. The inflammatory tumorigenesis required CD4 T cells, but not the T$_H$1 or T$_H$17 subsets. Deficiencies in IL-4 and IL-13 or IL-4 receptor α broke the link between inflammation and initiation of tumorigenesis. This study establishes the causality of CTLA4 insufficiency in gastric cancer and uncovers a role of type 2 inflammation in initiating gastric epithelial transformation. These findings suggest possible improvement of immune therapies by blocking tumorigenic type 2 inflammation while preserving antitumor type 1 immunity.

INTRODUCTION

Gastric (stomach) cancer (GC) is the second most lethal and the fourth most common cancer, causing more than 700,000 deaths per year worldwide (Lozano et al., 2012). GC is usually diagnosed at age 60 yr or older, with a higher risk in minorities. However, a recent study found an upward trend in incidence of noncardia GC (which refers to GC in all areas except the top part of stomach) in young white Americans (ages 25–39 yr; Anderson et al., 2010). GC represents a prototype of inflammatory carcinogenesis in solid tumors. Indeed, it is the study of GC that has provided some of the early evidence for the role of inflammation in cancer development. GC often develops occultly until a sign of metastatic cancer emerges, such as the "telltale" lymph node metastasis termed Virchow's node (Siosaki and Souza, 2013), which is named after Virchow, who made the original observation in the 19th century and also proposed the link between inflammation and cancer.

Gastric adenocarcinoma (GA) accounts for most GC cases. Its origin remains unclear. In a classical paradigm known as the Correa cascade, the etiology of GA is described as a histopathological process proceeding from gastritis, intestinal metaplasia (IM), and dysplasia to carcinoma (Correa, 1988). A new type of gastric metaplasia, spasmolytic poly-

peptide-expressing metaplasia (SPEM), possibly a precursor of IM, has been identified as a premalignant pathology in the inflammatory process of human GA (Goldenring et al., 2010). Multiple types of inflammatory signals are implicated in GA (Fox and Wang, 2007). These signals may originate from autoimmune responses (such as in pernicious anemia caused by autoimmunity against parietal cells; Toh et al., 1997) or immune damage associated with microbial infection. The most recognized GC risk factor is *Helicobacter pylori* (Wroblewski et al., 2010). Most cases of *H. pylori* colonization likely occurred in childhood. It has been estimated that GC develops in ~1% of *H. pylori*–infected individuals (Imrie et al., 2001). Substantial variations exist in the association between GC and *H. pylori*, which may be attributable to distinct *H. pylori* strains and host variability. The etiology of GC likely involves complex interactions between environmental and host-intrinsic factors.

Host factors for GC are not well understood. Among the few host genes implicated in GC development, the most perplexing is perhaps *CTLA4*. A recent clinical case report showed that *CTLA4* haploinsufficiency (heterozygous null mutations) led to GC in >10% (3/24) of the patients (Schubert et al., 2014; Zeissig et al., 2015; Hayakawa et al., 2016). In humans, heterozygous *CTLA4* null mutations may lead to CTLA4 reduction in T cells to <50% of con-

---

trols (~30% in mRNA and ~18–46% in proteins; Kuehn et al., 2014). Genetic studies of 251 cases of human GA from different ethnic populations have also found a paradoxical association with *CTLA4* because the risk alleles of *CTLA4* promoter and exon 1 linked to GC (Hadinia et al., 2007; Hou et al., 2010) are known to cause reduced CTLA4 expression (Ligers et al., 2001; Anjos et al., 2002; Wang et al., 2002). Of note, GC was also found in a patient with a deficiency of LRBA (LPS-responsive vesicle trafficking, beach- and anchor-containing) protein (Bratanič et al., 2017), a defect that causes secondary CTLA4 loss (Lo et al., 2015). CTLA4 is an immune checkpoint controlling T cell homeostasis (Tivol et al., 1995; Waterhouse et al., 1995; Chambers et al., 1997). It is a prototypical inhibitor of antitumor immunity (Chambers et al., 2001). Although the genetic evidence of CTLA4 insufficiency in human GC etiology is paradoxical to the prototypical role of CTLA4 in antitumor immunity, the new data are conceptually consistent with the inflammatory etiology of human GC in general and suggest new pathways of inflammatory tumorigenesis in humans.

We have created transgenic CTLA4 shRNA knockdown (CTLA4KD) mice to mimic CTLA4 insufficiency in humans. The transgene encodes a CTLA4-specific shRNA driven by a U6 promoter and reduces CTLA4 expression to ~40% of controls. This model has been used to study how CTLA4 insufficiency impacts immune regulation in various genetic backgrounds (Chen et al., 2006; Miska et al., 2012, 2014; Devarajan et al., 2014). We adapted the CTLA4KD model to study the role of CTLA4 insufficiency in GC development. We found that CTLA4 insufficiency, modeled by CTLA4KD or antibody blockade, caused the initiation of inflammatory tumorigenesis in the stomach of mice with susceptible genetic backgrounds. Furthermore, this study also provides the first evidence, to our knowledge, for a novel role of T_H2 cytokines IL-4/IL-13 in causing premalignant differentiation in gastric epithelia and thus mediating the link between inflammation and initiation of gastric tumorigenesis.

RESULTS
CTLA4 insufficiency modeled by transgenic RNA interference (RNAi) initiated the SPEM premalignancy development in the stomach

To understand the human GC genetic risks linked to CTLA4 insufficiency, we used the CTLA4KD mouse model. We first studied the animals on the BALB/c × C57BL/6 (B6) F1 mixed genetic background (called CB6F1). CB6F1 mice are a robust model with a noninbred yet homogenous genetic makeup (Miller et al., 2005). The CTLA4KD and PL4 vector control transgenic lines on the B6 genetic background (CTLA4KD/B6 or PL4/B6; Miska et al., 2012, 2014) were crossed with BALB/c mice to generate CTLA4KD mice and PL4 controls on the CB6F1 genetic background. Transgene-negative littermates were also used as controls. Supporting the genetic associations of CTLA4 insufficiency with human GC, CTLA4KD mice exhibited a type of gastric pre-

malignant pathology termed SPEM. As shown in Fig. 1, inflammatory infiltration in the stomach mucosa of CTLA4KD mice was detectable at 3 wk of age, and SPEM started to develop at 4 wk of age. At ~20 wk of age, all CTLA4KD mice exhibited extensive SPEM (100% penetrance; Fig. 1, A–C). Gross examination of the stomach identified a "wrinkled" appearance of the external surface (Fig. S1, A and B). At the mucosal surface, enlarged rugae were readily visible (Fig. S1 C); histological examination revealed massive SPEM (Fig. S1, D–G). CTLA4 insufficiency induced SPEM on the B6 genetic background, but it occurred mildly, with a late onset, and only developed in some animals; however, CTLA4 insufficiency induced robust SPEM pathology in mice on the BALB/c inbred genetic background (Fig. S1, H and I).

SPEM spontaneously progressed to adenocarcinoma with age in mice with CTLA4 insufficiency

GC development perhaps represents one of the clearest examples of age-associated carcinogenesis. We examined the impact of age on GC development in CTLA4KD mice. The SPEM lesion in this model persisted until ~52 wk of age, but by ~78 wk of age, all mice had dysplastic lesions in the gastric mucosa exhibiting cytological atypia and architectural complexity. Moreover, the frankly malignant pathology was evident with destructive growth beyond the mucosa that breached through the muscularis mucosae, with growth in the submucosa and even the muscularis externae. The cancerous growth had 100% penetrance and mainly consisted of adenocarcinoma with differentiated glandular structure, although heterogeneous neoplastic tissues could be identified (Fig. 1, A and C; and Fig. S2 A). Of note, human GC may manifest as well-differentiated adenocarcinoma (Kushima et al., 2006; Yao et al., 2006), including the GC associated with CTLA4 insufficiency (Hayakawa et al., 2016), which was unexpectedly more resistant than poorly differentiated GA to chemotherapy drugs (Maehara et al., 1987).

Besides pathological characterization, we also assessed the mucosal tumors in the CTLA4KD mice with biological tests. We made a cell line from an aging CTLA4KD mouse, which formed tumors in recipient mice (Fig. S2 B). Furthermore, we tested freshly isolated mucosal cells by implanting them subcutaneously into new recipient mice on the CB6F1 background. Gastric mucosal cells from aging CTLA4KD mice, but not the age-matched controls, formed tumors after injection into new recipients on the CB6F1 background (Fig. 1, D and E), confirming their transformed and immortalized status. Reflecting a feature of the original tumors (Fig. 1 A) in CTLA4KD mice, the new subcutaneous tumors that formed from the implanted cells had secretory glands (Fig. 1 F).

SPEM is characterized by overexpression of Trefoil factor 2 (TFF2; Goldenring et al., 2010), whereas loss of TFF1 causes GC (Soutto et al., 2011). In gastric mucosae of CTLA4KD mice, *Tff1* gene expression was substantially lower than controls, whereas *Tff2* gene expression was increased as

A

Controls | CTLA4KD mice

low power | high power | low power | high power

Age: 3wk
Inflammation

Age: 4wk
SPEM

Age: ~20wk
SPEM

Age: ~52wk
SPEM

Age: ~78wk
Neoplasia (GA)

B

Inflammation

| ** | * | ** | * | ** |

Ctrl KD | Ctrl KD | Ctrl KD | Ctrl KD | Ctrl KD

Age: 3 wk | 4 wk | ~20 wk | ~52 wk | ~78 wk

C

Metaplasia (SPEM)

| | * | ** | * | ** |

Neoplasia

Ctrl KD | Ctrl KD | Ctrl KD | Ctrl KD | Ctrl KD

Age: 3 wk | 4 wk | ~20 wk | ~52 wk | ~78 wk

D

CTLA4KD or WT
mouse mucosal cells

↓

Implant to
CB6F1 mice →

New Tumor

mm

E

***

Tumor Diameter (mm)

Ctrl KD

F

much as ~10-fold over controls (Fig. S3 A). We also assessed the mRNA expression of 84 genes commonly associated with cancer development and found that many genes exhibited no substantial changes in expression, whereas some had moderate alteration in the expression in the tumor at ~78 wk of age (not depicted). Furthermore, we assessed the expression of a few genes from the early to late stages of tumor development. We detected subtle or no changes in *Myc* and *p53* expression but found a dynamic profile of *Mmp9* as well as cell cycle control genes *Ccna1* and *Cdkn1c* (which have been associated with human GC; Sapari et al., 2012; Loh et al., 2014) along the inflammatory oncogenic cascade, especially during the transition from SPEM to GA (Fig. S3, B–E). Therefore, with the histological phenotype, the characteristic gene expression and the spontaneous progression to malignancy, the SPEM induced by CTLA4 insufficiency indeed represents a premalignancy.

CTLA4 insufficiency modeled by anti–CTLA4 antibody blockade induced the SPEM premalignancy in mice

To corroborate the role of CTLA4 insufficiency in gastric tumorigenesis by methods independent of RNAi, we treated mice on the CB6F1 background with anti–CTLA4 mAbs to down-modulate CTLA4. To recapitulate genetically predisposed CTLA4 insufficiency, mice were treated with anti-CTLA4 antibodies from 3–4 d of age for 4 wk and analyzed 1 wk after the treatment. The treatment induced obvious alteration detectable from the external surface (Fig. 2 A) and the luminal (mucosal) side of the stomach (Fig. 2 B), as well as inflammatory infiltration and characteristic SPEM pathology (Fig. 2, C–E) in the stomach in five of seven treated animals. The data corroborate the observations of gastric tumorigenesis in CTLA4KD mice and are consistent with the association of CTLA4 insufficiency with human GC.

Gastric tumorigenesis caused by CTLA4 insufficiency was caused by host–intrinsic immune dysregulation rather than microbiota

To investigate whether undetected overgrowth of normal floral *Helicobacter* contributed to the gastric tumorigenesis in CTLA4KD mice, we purified DNA from stomach samples and conducted a group-specific PCR assay for the *16S rRNA*

gene of all known *Helicobacter* species or for all bacteria. As shown in Fig. S4 (A), *Helicobacter 16S rDNA* was detectable in the gastric mucosa of normal mice. Both pan–*Helicobacter 16S rDNA* and pan-bacterial *16S rDNA* assays indicated a lower bacterial load in the gastric mucosa of CTLA4KD mice surveyed up to ~80 wk of age, suggesting that the gastric tumorigenesis in CTLA4KD mice occurred independently of pathogenic *Helicobacter* infections.

We next tested whether microbiota was required for the gastric tumorigenesis. CTLA4KD mice were rederived and maintained in germ-free (GF) facilities. The animals were analyzed at 9–10 wk of age. Similar to age-matched CTLA4KD mice maintained in specific pathogen–free (SPF) facilities, GF CTLA4KD animals developed extensive SPEM in the gastric mucosa (Fig. 3, A and B). Therefore, microbiota was not required for the initiation of tumorigenesis by CTLA4 insufficiency, although we cannot rule out the effect of potential microbial products in the sterilized food because it was not synthetic. Indeed, microbiota-independent autoimmune responses were evident in both cellular and humoral immune responses. There was a high titer of serum autoantibodies against gastric mucosa in CTLAKD mice even in the absence of microbiota (Fig. 3, C and D). Likewise, heightened T_H1, T_H2 and T_H17 responses were detected in CTLA4KD mice regardless of the GF or SPF conditions (Fig. 3 E and Fig. S4, B–D). Together, these results indicate that the intrinsic immune dysregulation induced by CTLA4 insufficiency was sufficient to cause de novo tumorigenesis in this model, although the results do not rule out the contribution of microbial agents in GC development.

Gastric tumorigenesis induced by CTLA4 insufficiency was transferrable with immune cells and required CD4 T cells

To examine whether the effect of CTLA4 insufficiency on gastric tumorigenesis indeed originated from immune cells, we reconstituted neonatal immunodeficient ($Rag1°$) mice with 15 million spleen cells from CTLA4KD or littermate control donors. Reconstituted animals were analyzed 6–10 wk later. Indeed, CTLA4KD donor cells, but not the controls, caused SPEM in reconstituted $Rag1^{o/o}$ recipients (Fig. 4 A). Depletion of CD4 T cells, but not CD8 cells, abrogated the inflammatory tumorigenesis by CTLA4KD donor cells

---

Figure 1. CTLA4 insufficiency modeled by RNAi transgenesis caused spontaneous initiation of SPEM and age–associated progression to malignancy in the stomach mucosae of CTLA4KD mice. CTLA4KD mice and wild-type littermates from ~3 to ~78 wk of age were analyzed for gastric histopathology. **(A)** Representative images of H&E-stained sections (a low-power magnification image followed with a high-power image of the highlighted area). The arrow (top right) indicates inflammatory infiltrates in 3-wk-old CTLA4KD mice. **(B and C)** Histopathology scores of gastric inflammation, SPEM, and neoplasia. Data represent four to seven mice for each 3-wk group pooled from two experiments, four mice for each 4-wk group pooled from two experiments, five mice for each ~20-wk group pooled from two experiments, four mice for each ~52-wk group from two cohorts in one experiment, and 6 mice for each ~78-wk group pooled from three experiments (mean ± SEM; Mann–Whitney test). **(D–F)** Verification of the transformed and immortalized status of the gastric mucosal cells in the CTLA4KD model. The mucosal cells from CTLA4KD or control mice at ~80–90 wk of age were implanted into CB6F1 recipients. Tumors formed in ~1 wk in recipients of CTLA4KD donor cells, but not controls (D). The sizes of tumors from cell implants were estimated by diameter measurement (E). H&E sectioning revealed that the implanted tumors had secretory glands (F), a feature of the original gastric tumor. Bars: (low power) 500 µm; (high power) 100 µm. Data represent five to seven mice pooled from two experiments (mean ± SEM; Student's *t* test). *, P < 0.05; **, P < 0.01; ***, P < 0.001.
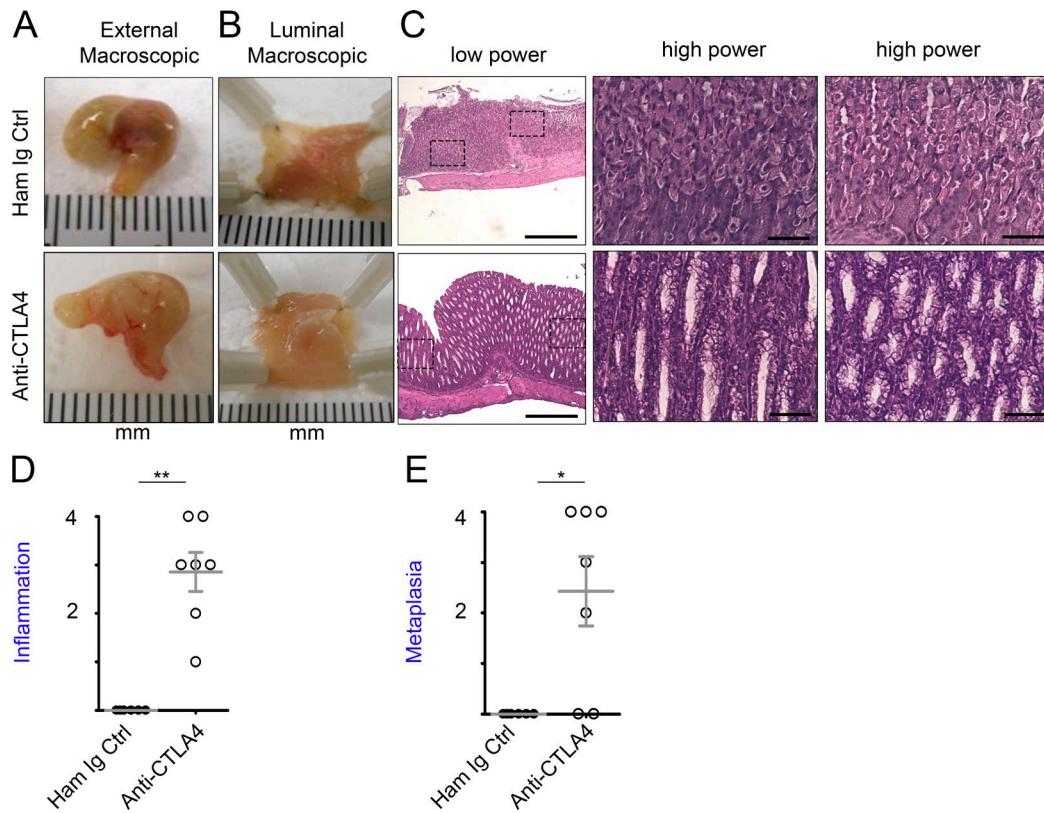
Figure 2. **CTLA4 insufficiency modeled by anti–CTLA4 monoclonal antibody blockade induced SPEM in wild-type mice.** Wild-type mice on the mixed CB6F1 background were treated with monoclonal antibodies against CTLA4 or control, from 3–4 d of age for 4 wk. The animals were analyzed at 5 wk of age. **(A)** Images of external stomach. **(B)** Images of the luminal side in the stomach. **(C)** Representative images of H&E-stained sections (low-power images followed with high-power images of the highlighted areas). Bars: (low power) 500 µm; (high power) 100 µm. **(D and E)** Summary of histopathology scores. Data represent six to seven mice in each group pooled from two experiments. Each data point represents one animal (mean ± SEM; Mann–Whitney test). *, P < 0.05; **, P < 0.01.

(Fig. 4, B–D). We then conducted the adoptive transfer experiment with a mixture of $CD25^-$ spleen cells from CTLA4KD donors with the $CD25^+$ fraction from the spleen of normal mice, or vice versa. The former, but not latter, group exhibited inflammation and SPEM in the stomach (Fig. 4, E and F), strongly suggesting that the defect of CTLA4 insufficiency that causes de novo inflammatory tumorigenesis resides in the $CD4^+CD25^-$ pathogenic effector T (T_{eff}) cell rather than regulatory T (T_{reg}) cell subset. Of note, the role of $CD4 T_{eff}$ cells is unlikely to be caused by their helper function for antibody production because serum transfer from CTLA4KD donors did not cause pathology in the stomachs of recipient mice (not depicted).

T_H1 and T_H17 cells were not required for tumorigenesis caused by CTLA4 insufficiency

To examine the role of T_H1 cells in inflammatory tumorigenesis caused by CTLA4 dysregulation, we used IFN-γ–deficient mice on the BALB/c background. Anti-CTLA4 mAb initiated SPEM efficiently in mice on the BALB/c background. IFN-γ deficiencies did not inhibit the extent of inflammatory

pathology or SPEM development (Fig. 5 A), indicating that T_H1 responses were not required for the initiation of inflammatory tumorigenesis caused by CTLA4 insufficiency.

We then tested the role of T_H17 cells. In our models, IL-17A rather than IL-17F was detected at a high levels. Therefore, we used IL-17A knockout mice to study the role of T_H17 cells. As shown in Fig. 5 B, deficiencies in IL-17A did not reduce inflammatory infiltration in the gastric mucosa. Importantly, IL-17A knockout did not curtail the initiation of tumorigenesis, as the extent of SPEM between CTLA4KD IL17A$^+$ and CTLA4KD IL17A^o mice did not differ significantly (Fig. 5 B).

IL-4 and IL-13 played an essential role in mediating the link between inflammation and initiation of tumorigenesis

Because our original hypothesis on the causal role of T_H1 and T_H17 cells in the inflammatory tumorigenesis turned out to be incorrect (Fig. 5), we examined a potential role for T_H2 dysregulation in gastric tumorigenesis. IL-4 and IL-13 are essential for T_H2 differentiation and effector function (Ansel et al., 2006). The *IL4* and *IL13* genes are located in adjacent
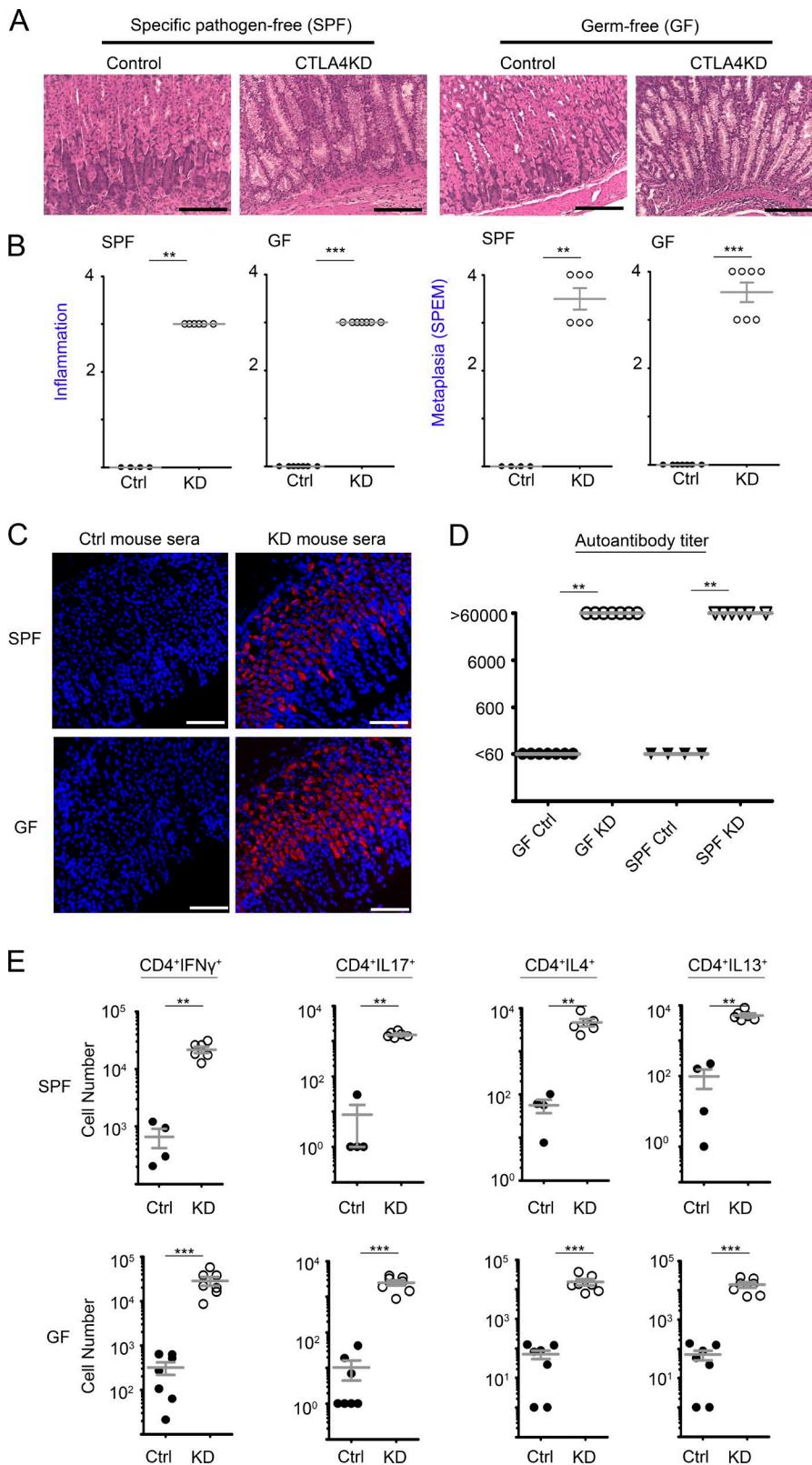
Figure 3. Gastric tumorigenesis initiated by CTLA4 insufficiency occurred independently of microbiota, with evidence of autoimmunity against gastric mucosal tissue. CTLA4KD mice and controls in SPF versus germ-free (GF) facilities were analyzed between 9–10 wk of age. **(A)** Representative histopathology images. Bars, 100 μm. **(B)** Summary of pathology scores (Mann–Whitney test). **(C)** Serum or plasma samples from CTLA4KD and wild-type littermates maintained in GF or SPF facilities were assayed for gastric mucosal autoantibodies. Autoantibodies that bound to gastric mucosal antigens were revealed by secondary antibodies conjugated with fluorescent probes (red); DAPI counterstained for nuclei (blue). Bars, 100 μm. **(D)** Titration of the autoantibodies (assay range, 60–60,000; Kruskal–Wallis test). **(E)** The lymphocytes from CTLA4KD and control mice were analyzed by intracellular cytokine staining. Summary of the total numbers of IFN-γ–producing T_H1, IL-17A–producing T_H17, and IL-4– or IL-13–producing T_H2 effector cells in the draining lymph nodes of CTLA4KD mice versus controls in SPF versus GF environments. Each data point represents one animal (mean ± SEM; Mann–Whitney test). For all panels, data represent four to seven mice pooled from two analysis experiments with mice from one GF derivation. **, P < 0.01; ***, P < 0.001.
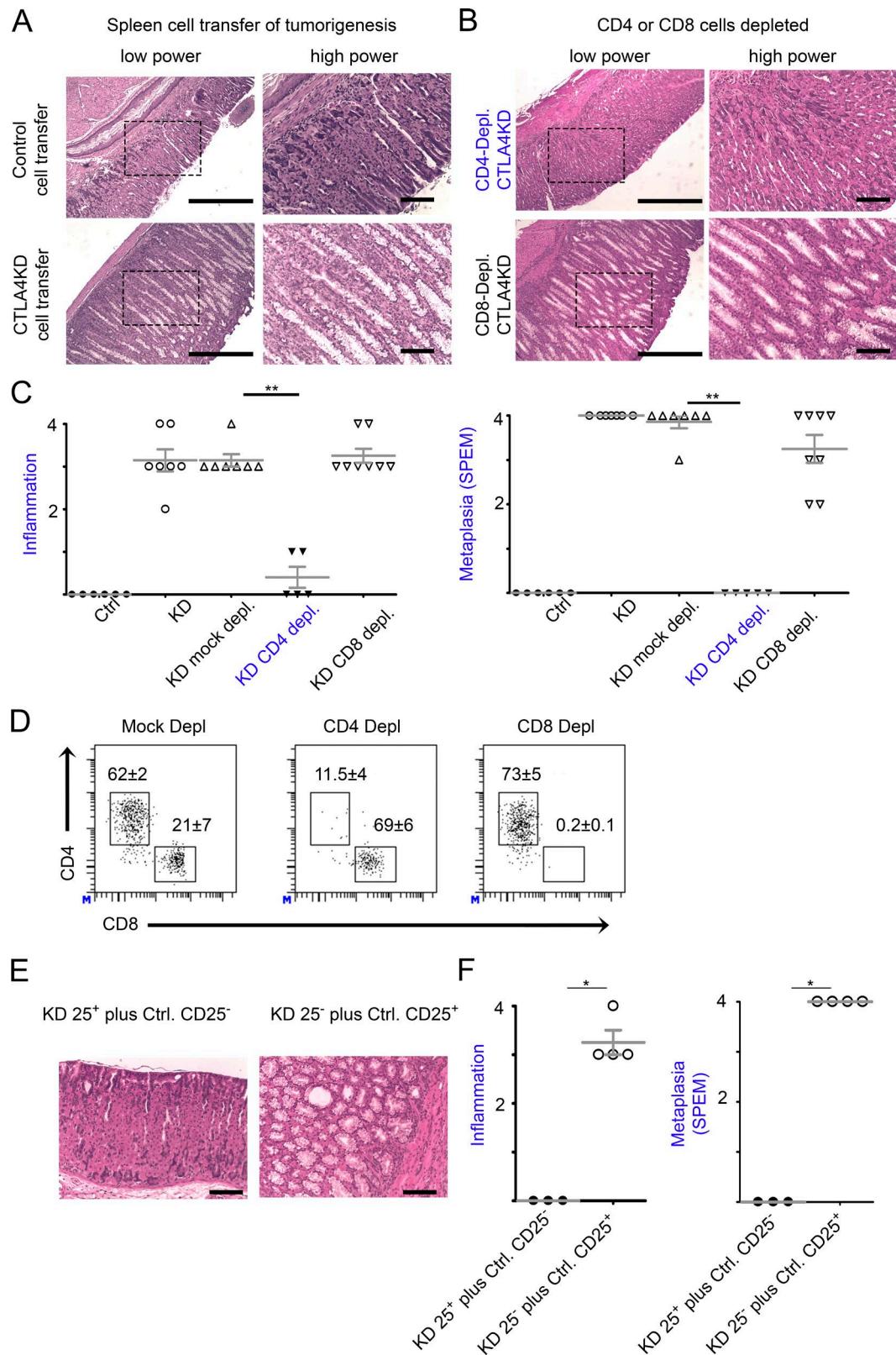
Figure 4.   **CD4 T cells were required for gastric tumorigenesis initiated by CTLA4 insufficiency.** Splenocytes, or CD4- or CD8-depleted fractions of splenocytes, were prepared from CTLA4KD or littermate control donors. For some experiments, splenocytes from CTLA4KD and normal mice were separated into CD25+ and CD25− fractions and cross-mixed at 1:25 ratio with CD25+ cells from CTLA4KD donors and CD25− cells from normal controls, respectively,

positions. Their functions overlap but are not completely redundant (Hallett et al., 2012; Wynn, 2015). Although IL-4/IL-13 dysregulation is implicated in cancer cell survival and proliferation (Hallett et al., 2012), whether it has a role in the early stage of tumorigenesis (i.e., the differentiation of premalignant lineages) remains unclear.

To obtain direct evidence for IL-4/IL-13 in the initiation of tumorigenesis, we used genetic ablation. Recently, a knockin line with loxP sites flanking the adjacent IL-4 and IL-13 genes (the IL4/IL13[flox] line) was generated and enabled conditional knockout of both IL-4 and IL-13 (Liang et al., 2011). In preliminary studies, we obtained IL4/IL13[flox] mice and crossed them with CMV-Cre mice to generate a line of germline knockout on both IL4 and IL13 genes, IL4/IL13°. This allowed us to assess the effect of complete deficiencies in both IL-4 and IL-13, in keeping with recent observations on the improved clinical activity against allergic conditions when both IL-4 and IL-13 were blocked (Gandhi et al., 2016). In the CTLA4KD model, IL4/IL13 deficiencies did not alter the population size of T_H1 or T_H17 subsets (Fig. S5 A). As shown in Fig. 6 A, although CTLA4KD IL4/IL13^{+} mice exhibited robust SPEM pathology, littermate CTLA4KD IL4/IL13° mice had no SPEM lesions in the stomach even at 8–10 wk of age, which otherwise would have developed at ∼4 wk of age (see Fig. 1). However, the extent of inflammatory pathology was comparable between CTLA4KD IL4/IL13° and CTLA4KD IL4/IL13^{+} littermates (Fig. 6 A). Indeed, destruction of parietal cells in the CTLA4KD IL4/IL13° mice was evident in histopathology (Fig. 6 A) and reflected in the elevated pH of gastric luminal fluid (not depicted).

The finding that IL-4/IL-13 deficiencies suppressed SPEM development prompted us to explore a potential therapeutic modality: neutralizing type 2 cytokines to block the initiation of inflammatory tumorigenesis. We tested anti–IL-4 antibody treatment in the CTLA4KD model. As shown in Fig. 6 B, although neutralizing IL-4 in CTLA4KD mice did not reduce the extent of inflammatory infiltration, it significantly inhibited SPEM pathology.

IL-4 and IL-13 may act directly on the epithelial compartment, or signal intrinsically in immune cells and indirectly affect epithelial transformation. As an initial assessment of this possibility, we obtained IL-4 receptor α (IL4Rα) knockout mice (Noben–Trauth et al., 1997). IL-4Rα is a subunit for both IL-4 and IL-13 receptors (Hallett et al., 2012). We crossed IL-4Rα° mice with a Rag° line and generated

IL4RaºRagº double knockout mice and IL4Rα[+]Ragº controls. These mice were used as recipients for adoptive transfer of spleen cells from CTLA4KD or control donors. The transferred spleen cells were not only capable of producing IL-4 and IL-13 but also had intact IL4Rα–mediated signaling. The reconstituted animals thus had IL4Rα deficiency or sufficiency in the stromal and epithelial lineages. To make the experiments more rigorous, the IL4RαºRagº mice or IL-4Rα[+]Ragº controls were reconstituted with spleen cells at either an adult age (Fig. 6 C) or neonatal age (Fig. 6 D). Indeed, IL4Rα deficiency in the recipient abrogated the initiation of tumorigenesis, but not the inflammation (Fig. 6, C and D). This effect was not caused by reduction in recruitment of transferred CTLA4KD T cells to the stomach mucosa. There were also similar frequencies of F4/80^{+} cells (macrophages; Fig. 6 E) or Gr1^{+} granulocytes (not depicted) in inflamed stomach mucosa of IL4Rα° or IL4Rα[+] recipients. Further studies with definitive lineage tracing tools are needed to pinpoint the IL4Rα signaling to a specific epithelial lineage in the stomach mucosa. However, it is worth noting that the predominant cells recruited to the stomach mucosa at this early stage were T cells, and the SPEM cells were likely differentiated from resident cells in the stomach, in particular, by transdifferentiation from chief cells (Nam et al., 2010). Collectively, these results strongly suggest that the inflammatory tumorigenesis is triggered by proximal "cross talk" between dysregulated T_H2 cells and epithelial cells, with a major role of IL4Rα–mediated signaling in the epithelial compartment, which initiates the early transformative events.

Inflammatory tumorigenesis caused by CTLA4 insufficiency was associated with epigenetic dysregulation reflected in human GC

Chronic cytokine stimulation may lead to epigenetic dysregulation. Indeed, IL-4 signaling has long been known to cause modification of DNA methylation and drive lineage specification of immune cells (Ansel et al., 2006). IL-4/IL-13 receptors are expressed by human GC cells (Morisaki et al., 1994) as well as in the SPEM and GA in the CTLA4KD model (Fig. S5 B). Thus, IL-4/IL-13 signaling may, directly or indirectly, contribute to epigenetic dysregulation that promotes GC development. One of the prominent epigenetic changes in a tumorigenic cascade is an altered profile of methylation in genomic DNA at the 5 position of cytosine (5mC; Jones, 2012). The abundance of 5mC in the genomes

---

or vice versa. The immune cells were used to reconstitute neonate immunodeficient Rag1° recipients at 12–15 × 10⁶ cells each. The recipients were analyzed 6–10 wk after the immune reconstitution. **(A)** Representative gastric pathology of mice receiving the whole splenocytes. **(B)** Representative gastric pathology of mice receiving the splenocyte preparations depleted of CD4 or CD8 T cells. Bars: (low power) 500 μm; (high power) 100 μm. **(C)** Summary of pathology scores. Data represent six or seven mice pooled from two total splenocyte transfer experiments and five to eight mice pooled from two fractioned splenocyte transfer experiments (mean ± SEM; Kruskal–Wallis test). Bars: (low power) 500 μm; (high power) 100 μm. **(D)** Flow cytometry verification of mice reconstituted with CD4- or CD8-depleted cells, showing the percentage of T cell subsets in the spleen. Data represent three to seven mice per group pooled from two experiments (mean ± SEM; P < 0.01, Student's t test). **(E and F)** Pathology assessment of the Rag1° mice reconstituted with CTLA4KD CD25^{+} plus normal CD25^{−} spleen cells or vice versa. Bars, 100 μm. Data represent three to four mice pooled from two experiments. Each data point represents one animal (mean ± SEM; Mann–Whitney test). *, P < 0.05; **, P < 0.01.
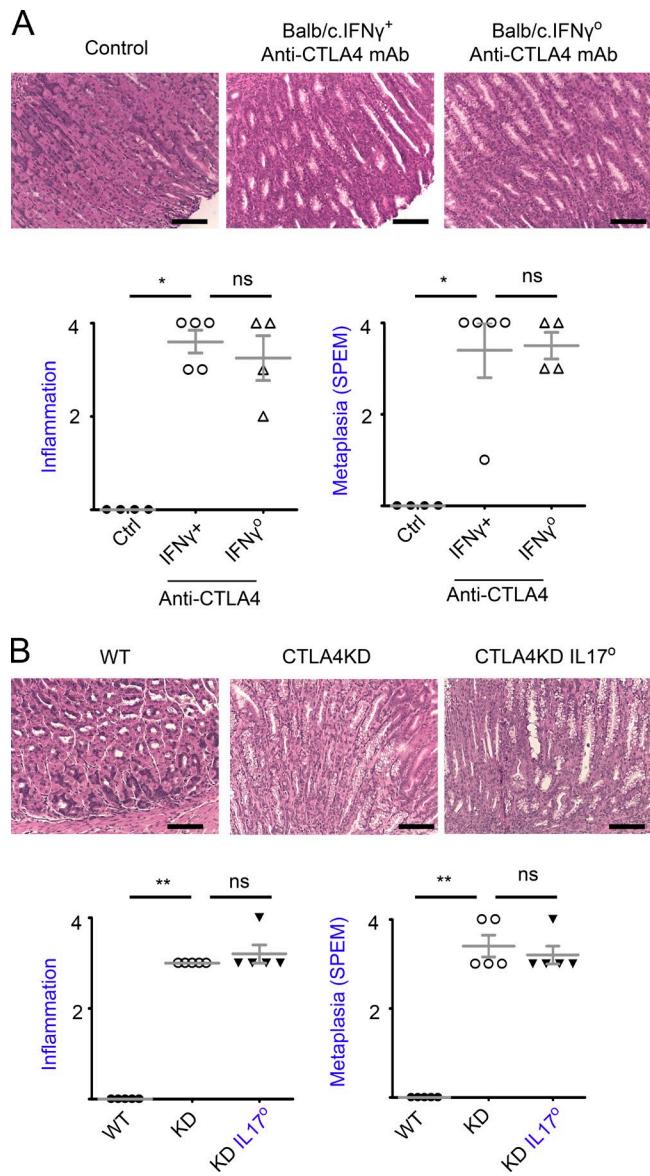
Figure 5. **Neither IFNγ nor IL17A was required for initiation of inflammatory tumorigenesis by CTLA4 insufficiency. (A)** Anti-CTLA4 antibodies were administered to IFNγ° or IFNγ+ mice on the BALB/c genetic background for 4 wk. The control Ig or vehicle treatment group was a pool of both IFNγ+ and IFNγ° mice. The animals were analyzed 1 wk after the mAb treatment. Representative gastric histopathology images (bars, 100 µm) are followed with a summary of pathology scores. Data represent four or five mice per group pooled from two experiments (mean ± SEM; Kruskal–Wallis test). **(B)** CTLA4KD IL17A°, CTLA4KD IL17A+, or wild-type littermates were analyzed at 7–26 wk of age. Representative gastric histopathology images (bars, 100 µm) are followed with a summary of pathology scores. Data represent five mice per group pooled from two experiments. Each data point represents one animal (mean ± SEM; Kruskal–Wallis test). *, P < 0.05; **, P < 0.01; ns, not significant.

makes 5mC content an insensitive parameter for quantifying changes. Prompted by a study of melanoma-associated loss of 5-hydroxymethylcytosine (5hmC; Lian et al., 2012), the hydroxylated product of 5mC, we quantified 5hmC content in genomic DNA of gastric mucosae from CTLA4KD mice and controls as a global assessment of methylation-based epigenetic changes (Fig. 7, A and B). We detected a lower 5hmC content in GC samples in aging CTLA4KD mice than in littermate controls, but not in the young groups. We examined regulatory genes in the 5hmC pathway, ten-eleven translocation methylcytosine dioxygenase (*Tet*) and isocitrate dehydrogenase (*Idh*) genes. We detected a consistent change of gene expression only in Idh2 throughout the progression from SPEM to GA, but there was a significant reduction of Tet3 expression at the early stage of tumorigenesis (Fig. S5 C). Interestingly, introducing IL-4/IL-13 deficiency into the CTLA4KD model restored Tet3 expression (Fig. 7 C) but did not rectify Idh2 dysregulation (Fig. 7 D). Therefore, the epigenetic dysregulation associated with inflammatory tumorigenesis caused by CTLA4 insufficiency may be contributed by IL-4/IL-13–dependent and independent mechanisms.

We examined 5hmC in human GC. We obtained GA samples and healthy stomach mucosal tissues and conducted 5hmC staining as described previously (Lian et al., 2012; Minor et al., 2013). As shown in Fig. 7 (E and F), the proportion of 5hmC+ nuclei was substantially reduced in GA cells compared with healthy controls. These results in human GC, taken together with the evidence from CTLA4KD mice, suggest that 5hmC dysregulation may be involved in gastric epithelial transformation driven by type 2 inflammation.

DISCUSSION

Control of autoimmunity requires critical immune checkpoints such as CTLA4, which regulates not only T cell homeostasis but also immune tolerance induction to specific self-antigens (Tivol et al., 1995; Waterhouse et al., 1995; Chambers et al., 1997; Ise et al., 2010). CTLA4 is well known as an archetypical inhibitor of antitumor immunity. As such, the concept that CTLA4 insufficiency can cause cancer is paradoxical to the basic tenet that blocking CTLA4 induces antitumor immunity. This paradox is real and relevant, however, as indicated by the association of CTLA4 insufficiency and GC in humans. The data from this study with animal models establish the causality of CTLA4 insufficiency in de novo cancer development in the stomach. CTLA4 modulation by RNAi silencing or antibody blockade in mice initiated spontaneous tumorigenesis in the stomach, without a requirement for microbiota, but is accompanied by autoimmune responses against gastric mucosal tissue. These results suggest a critical role of host-intrinsic immune dysregulation in the initiation of inflammatory tumorigenesis.

Epidemiological studies have associated autoimmune disorders with a variety of cancers in humans (Volkers, 1999;

A

WT   IL4/IL13°   CTLA4KD   CTLA4KD IL4/IL13°
low power
high power

B

WT   CTLA4KD Control   CTLA4KD Anti-IL4 mAb

C

Adult Rag° Recipients:
20 x 10⁶ KD mouse spleen cells
IL4Rα⁺Rag°   IL4Rα°Rag°

D

Neonate Rag° Recipients:

E

WT spleen cells → IL4Rα⁺Rag°
6±2%
129±50
36±3%
910±241

KD spleen cells → IL4Rα⁺Rag°

KD spleen cells → IL4Rα°Rag°
5±1%
160±69
34±6%
1661±1015

F4/80

TCRβ
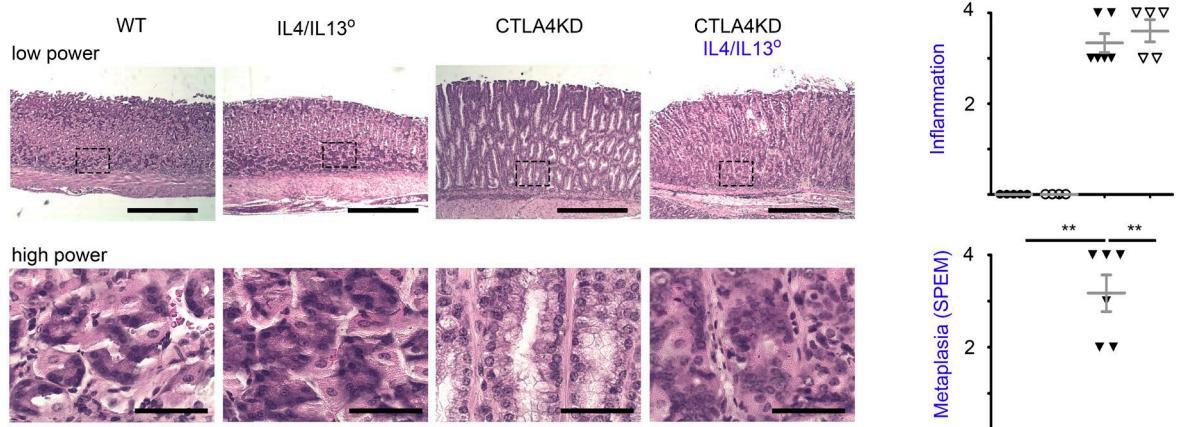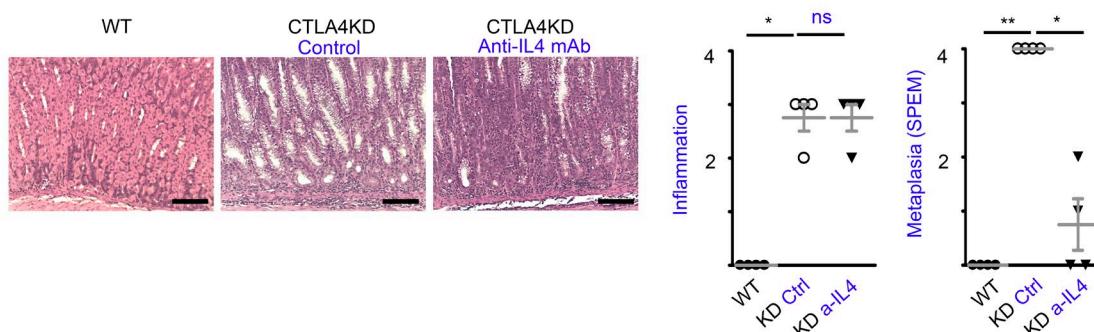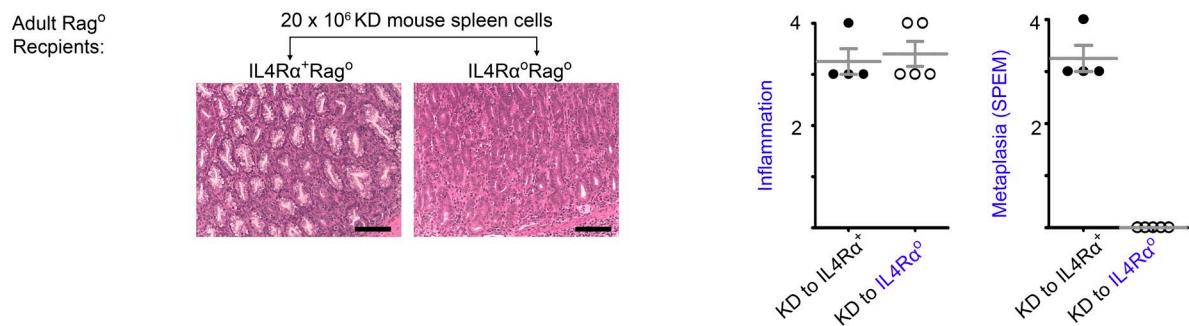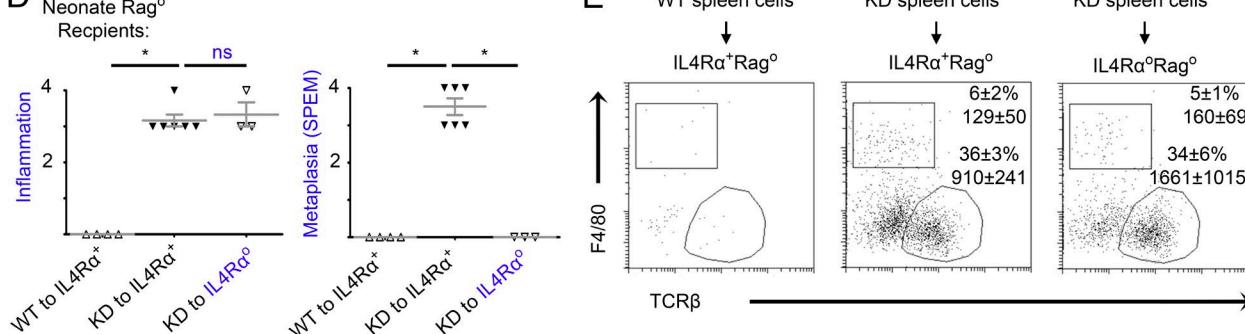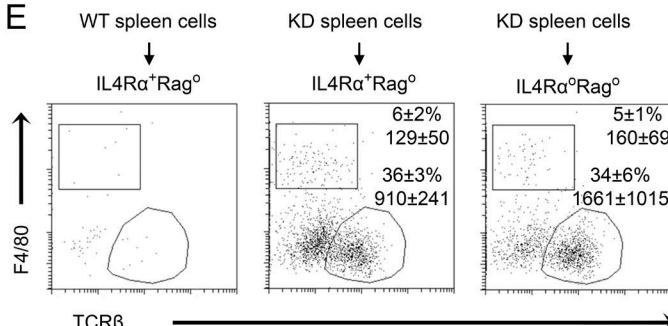
Hemminki et al., 2012). A study with a CD4 T cell receptor transgenic model has also demonstrated a causal role of autoimmunity in GC development (Nguyen et al., 2013). On the other hand, experimental and clinical evidence indicates that autoimmunity may function as an effector mechanism for tumor killing as well. Thus, autoimmunity can be a "double agent" in mediating either protumor or antitumor activities. Of note, it is increasingly recognized that autoimmune toxicity might be a critical barrier that limits cancer immunotherapy. Furthermore, inflammatory effectors induced by checkpoint blockade might underlie the clinical observations that in some cases, immunotherapy might exacerbate cancer progression (Toomer and Chen, 2014; June et al., 2017; Sharon, 2017). Which role autoimmunity assumes perhaps depends on the susceptible type of target cells in an inflammatory setting as well as the dominant types of immune effectors and inflammatory pathways.

In a broad stroke, immunity and immune-mediated inflammation are categorized into either type 1 or type 2 (Gause et al., 2013; Wynn, 2015; Gandhi et al., 2016). Refuting our original hypothesis, the data from our experiments show that it is not the type 1 immunity by IFN-γ–producing T_H1 or IL-17–producing T_H17 cells that causes tumorigenesis in this model, although it causes inflammation and tissue damage. Rather, it is the type 2 inflammation driven by IL-4/IL-13 that mediates the link between inflammation and initiation of tumorigenesis in this model of GC caused by immune dysregulation. Of note, suboptimal expression of CTLA4 in the CTLA4KD model does not compromise the in vivo and in vitro suppressive activity of $CD4^+Foxp3^+$ T_{reg} cells (Devarajan et al., 2014), although the presence of CTLA4 is required for T_{reg} cell function (Wing et al., 2008). Given the requirements for $CD4^+CD25^-$ T cells and IL-4/IL-13, a plausible conclusion is that IL-4/IL-13–producing T_H2 cells drive the initiation of GC development, although definitive evidence with cell-specific targeting is needed to pinpoint the exact source of IL-4/IL-13 that causes the inflammatory tumorigenesis. Furthermore, we should note that our conclusion on the requirement of IL-4/IL-13, but not IFN-γ and IL-17, is limited to the initiation phase in terms of SPEM differentiation. Many other cytokines have been well documented for their role in stomach cancer development; for example, IL-1β (Tu et al., 2008) and TNF-α (Oguma et al., 2008). Although neutralizing TNF-α or blocking IL-1R1 with in vivo antibody treatment did not inhibit inflammation or SPEM in CTLA4KD mice (unpublished data), further studies are needed to examine their role in the progression of inflammatory tumorigenesis.

T_H2 cells, through complex interactions with several subsets of innate immune cells, play a key role in driving type 2 immune responses, which are characterized by production of type 2 cytokines, including IL-4, IL-5, IL-9, IL-13, IL-25, and IL-33 (Gause et al., 2013; Wynn, 2015). The role of IL-4/IL-13–producing T_H2 cells and innate immune cells is well documented in facilitating tumor cells evading immune attack by antagonizing tumor-killing T_H1, T_H17, or cytotoxic T lymphocytes and/or promoting immunosuppressive myeloid cells. This has been demonstrated in breast cancer as well as in many other types of cancers as a shared mechanism driving tumor progression (Bronte et al., 2003; DeNardo et al., 2009; Gabrilovich and Nagaraj, 2009; Gocheva et al., 2010). Whether dysregulation of T_H2 cells may cause the early stage tumorigenic differentiation or cellular transformation has remained unclear, although observations have been made that in some cases of human GC associated with *H. pylori*, IL-4– or IL-13–producing T_H2 cells were associated with the transition from gastritis to dysplasia (Ren et al., 2001). Our study identifies an essential role for T_H2 cells in driving the differentiation of the SPEM premalignant lineage and thus initiating tumorigenesis. In addition, IL-4/IL-13 production by T_H2 cells is likely also involved in the progression from SPEM to cancer through the induced IL-4/IL-13 receptors in the epithelium, which remains to be examined with lineage-specific and time-controlled targeting.

It should be emphasized that the particular regimen of anti-CTLA4 treatment used in this study was purported to corroborate the effect of genetically predisposed CTLA4 insufficiency with a method independent of the RNAi approach. The relevance of the results to clinical anti-CTLA4 therapies cannot be determined. Anti-CTLA4 treatment has conferred remarkable benefits of cancer survival in patients. On the other hand, inflammatory toxicity was a common side effect, particularly in the gastrointestinal tract (Phan et al., 2003; Beck et al., 2006; Hodi et al., 2010). Both the upper and lower gastrointestinal tracts were affected. For example, in some patients who received anti-CTLA4 treatment

Figure 6. **IL–4 and IL–13 were required for initiation of inflammatory tumorigenesis by CTLA4 insufficiency. (A)** CTLA4KD IL4/IL13° mice (knockout of IL-4 and adjacent IL-13 genes) were analyzed at 8–10 wk of age in comparison to three types of littermate controls: wild-type, IL4/IL13°, and CTLA4KD(IL4/IL13⁺). Data represent four to six mice per group pooled from two experiments (mean ± SEM; Kruskal–Wallis test). Bars: (low power) 500 µm; (high power) 50 µm. **(B)** CTLA4KD mice were treated with anti–IL-4 mAb for 4 wk and analyzed at 5–6 wk of age. Data represent four mice per group pooled from two experiments (mean ± SEM; Kruskal–Wallis test). Bars, 100 µm. **(C and D)** IL4Rα°Rag° mice or IL4Rα⁺Rag° controls at 6 wk (C) or 2–3 d of age (D) were reconstituted with 20 × 10⁶ splenocytes from CTLAKD or normal mice and analyzed 5–6 wk later. Representative gastric histopathology images (bars, 100 µm) are followed with a summary of pathology scores. Data represent three to six mice per group pooled from two experiments. Each data point represents one animal (mean ± SEM; Mann–Whitney test in C and Kruskal–Wallis test in D). **(E)** Flow cytometry analyses of IL4Rα°Rag° and IL4Rα⁺Rag° mice reconstituted with spleen cells (groups shown in D) for immune cell profile in the stomach mucosa. The plots are gated on live cells (identified by viability dye), showing percentage of αβ T cells and macrophages of the CD45⁺ population, and the total number of the gated population recovered from approximately one fourth of the stomach mucosa used for flow cytometry. *, P < 0.05; **, P < 0.01; ns, not significant.
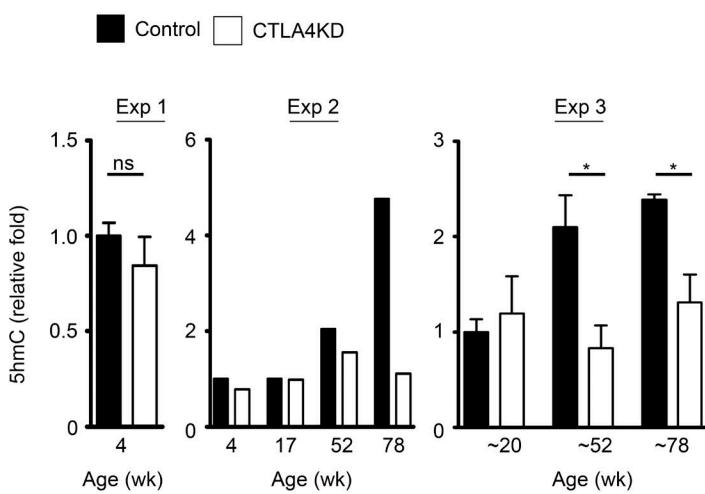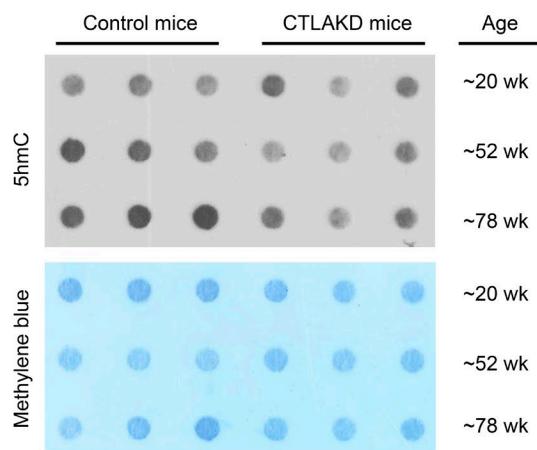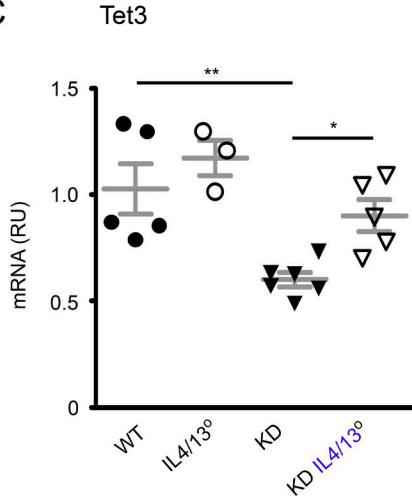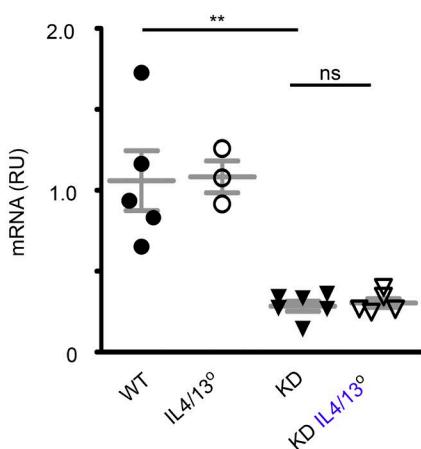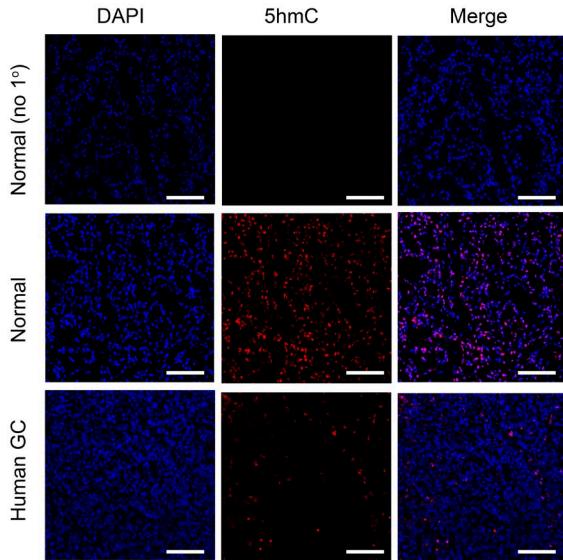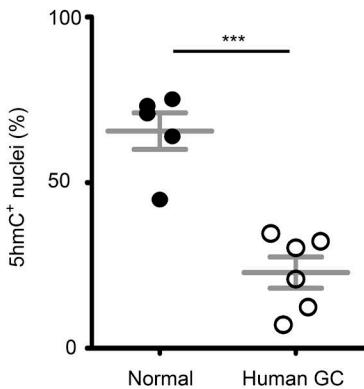
and underwent esophagogastroduodenoscopy with biopsies, inflammatory pathology in the stomach was identified by histological analyses, although in general, enterocolitis was detected more frequently than gastritis (Beck et al., 2006). Whether and how the de novo carcinogenic effect uncovered in our study has any relevance to clinical anti-CTLA4 therapies remains to be assessed in the future. Nevertheless, as cancer immunotherapy becomes a mainstay, the long-term effect of autoimmune-derived inflammatory signals that arise from deactivating immune tolerance mechanisms may need to be studied. It may also be worth noting that clinical trials with anti-CTLA4 treatment did not show benefit in GC patients. Human GC cell lines, similar to the mouse GC in the CTLA4KD model, express functional IL-4 receptor (Morisaki et al., 1994; Essner et al., 2001). Blocking a critical immune checkpoint gene such as CTLA4 unleashes a "mixed bag" of both type 1 and type 2 inflammatory effectors. The data from this study suggest possible improvement of immune therapies by blocking IL-4/IL-13–mediated protumor type 2 inflammation while preserving antitumor type 1 immunity.

Overall, the data from this study are consistent with the premise that type 1 immunity in general is geared toward tissue destruction, whereas type 2 immunity is more attuned to damage repairing (Gause et al., 2013; Wynn, 2015). In that regard, de novo tumorigenesis in a setting of chronic type 2 inflammation perhaps represents an aberrant process of tissue repairing driven by IL-4/IL-13, at least in some solid organs. CTLA4KD mice not only model GC caused by CTLA4 insufficiency but also capture a converging point of inflammation and a shared process of histopathological progression from premalignancy (SPEM) to cancer (GA), regardless of whether the original initiator of inflammatory tumorigenesis is extrinsic microbes such as *Helicobacter* species or intrinsic immune dysregulation.

Collectively, the results from this study suggest de novo tumorigenesis driven by immune dysregulation. In brief, CTLA4 insufficiency causes chronic inflammation, with T_H2 responses and heightened production of IL-4/IL-13 triggering Tet3-mediated epigenetic dysregulation, whereas other inflammatory effectors drive IL-4/IL-13–independent hits. This process leads to an altered programing of gene expression that initiates epithelial transformation and the differentiation of premalignant cells. Data from the GF experiment suggest that host-intrinsic autoimmunity can be sufficient in initiating this pathway of tumorigenesis, although microbiota or infectious agents may likely provide additional inflammatory stimuli.

Similar to other highly lethal cancers, GC has a poor prognosis. Therefore, the key to lowering the burden of this disease may lie in prevention of malignant development. This study suggests a scenario of distinct roles played by a genetic risk followed by an epigenetic abnormality in the gastric carcinogenic cascade. First, genetically determined or predisposed CTLA4 insufficiency or other types of immune dysregulation may cause autoimmune responses against gastric mucosal tissue in susceptible individuals; chronic stimulation by type 2 cytokines and other inflammatory effectors may then lead to metaplastic and premalignant differentiation through epigenetic reprogramming. Second, the premalignant lesion can be sustained in the setting of chronic inflammation, but yet-to-be-identified factors associated with aging may promote its progression to cancer. This progression may be further contributed by a failure to activate epigenetic up-regulation that promotes healthy aging and protects against cancer development. One might speculate that the well-documented mechanisms of type 2 cytokines in epigenetic programming of immune cells (Ansel et al., 2006) may be similarly involved in the epigenetic dysregulation of epithelial lineages in chronic inflammation. Furthermore, CTLA4 insufficiency caused by common genetic polymorphisms may also contribute to age-associated inflammatory tumorigenesis in the general population. Overall, the insight gained from this study may help develop new approaches for monitoring de novo tumorigenesis in high-risk populations with autoimmune conditions. The knowledge will also help propel new strategies of intervention to eliminate premalignant lesions or halt their progression when they are detected, thus preventing cancer development or recurrence.

MATERIALS AND METHODS
Mice
CTLA4KD and PL4 transgenic controls were described previously (Chen et al., 2006; Miska et al., 2012, 2014). The animals in this study were on a B6, BALB/c, or CB6F1 mixed background. IFNγ°, IL17A°, IL4/IL13^{flox}, CMV-Cre, Rag1°

Figure 7. **Inflammatory carcinogenesis in the stomach of mice with CTLA4 insufficiency was associated with epigenetic dysregulation in the 5hmC pathway. (A)** Relative quantification of 5hmC content in DNA from stomach mucosal tissue of CTLA4KD mice and littermate controls (experiment 1, *n* = 2–3 mice in each group; experiment 2, each bar represents one animal; experiment 3, *n* = 3 mice in each group, mean ± SEM). **(B)** Representative dot-blot of 5hmC staining of genomic DNA (top) compared with methylene blue staining of DNA (loading control). **(C and D)** mRNA expression of epigenetic regulatory genes Tet3 and Idh2 in gastric mucosal tissue samples of 8- to 10-wk-old CTLA4KD IL4/IL13° mice in comparison to wild-type, IL4/IL13° and CTLA4KD(IL-4/IL-13$^+$) controls. RU, relative units. Data represent three to six mice per group pooled from two experiments. Each data point represents one animal (mean ± SEM; ANOVA). **(E and F)** 5hmC staining in human GC (adenocarcinoma). Cryosections of frozen GC samples and controls were stained for 5hmC (Red). Results are representative of five normal mucosal samples and six GC samples. Representative staining is shown in C (top panels, no 1° Ab staining control of normal tissues; middle and bottom panels, 5hmc staining of healthy and tumor tissue sections, respectively). DAPI counterstained cell nuclei (blue). Bars, 100 μm. Percentages of 5hmC$^+$ nuclei in the normal versus GC group, with a total of 7,230 and 7,434 nuclei randomly sampled, respectively (*n* = 5–6 tissue samples; mean ± SEM; Student's *t* test), are summarized in D. Data represent two experiments. Each data point represents one sample. *, P < 0.05; **, P < 0.01; ***, P < 0.001.

mice were from The Jackson Laboratory. The IL4/IL13[flox] mice were crossed with CMV-Cre mice to generate germline deletion of both IL-4 and IL-13 genes. GF CTLA4KD mice were rederived by embryo transfer at Taconic. Other animals were maintained in an SPF barrier facility. The studies were approved by the Institutional Animal Care and Use Committee at the University of Miami.

Antibody treatment
Anti-CTLA4 antibodies (clone UC10-4F10-11) or controls (hamster Ig or PBS vehicle) were injected intraperitoneally into BALB/c or CB6F1 mice, at a dose of 30 μg per gram body weight, biweekly for 4 wk. The same schedule was used for treatments with anti–IL-4 mAbs (clone 11B11) at a dose of 40 μg per gram body weight. The animals were analyzed at 5–6 wk of age.

Adoptive transfer of immune cells
Sterile cellular preparations were made with the spleen of CTLA4KD/CB6F1 and littermate control donors. $15–20 \times 10^6$ splenocytes, or equivalent numbers of cells depleted of CD4^{+} or CD8^{+} cells, were used to reconstitute neonate Rag1° mice on the CB6F1, BALB/c, or B6 genetic background. In some experiments, the total splenocytes were separated into CD25^{+} and CD25^{−} fractions. Based on the typical yield at 1:25 ratio from the separation procedure using antibody and magnetic beads, a mixture of the CD25^{+} and CD25^{−} fractions was made at 1:25 ratio with splenocytes from CTLA4KD donors and littermate controls, respectively, or vice versa. Each Rag1° recipient was reconstituted with the mixture with a total 12 $\times 10^6$ cells at 2–3 d of age. Mice were analyzed 6–10 wk later.

Histopathology
Stomach samples were fixed in 10% formalin solution. Paraffin-embedded sections and H&E staining were done by the Pathology Research Resource Core at the University of Miami. Images were taken with a Vistavision microscope (VWR) or with an Olympus BH-2 microscope. The inflammatory infiltration in the CTLA4KD model is mainly limited to the submucosa and basal area of the mucosa. It is scored according to the following criteria: scores 1, 2, 3, and 4 indicate that <10%, 10–49%, 50–90%, and >90%, respectively, of the length of the tissue sections was affected by inflammatory infiltration along the stomach sections with mucosal tissues. SPEM or neoplasia is scored as follows: scores 1, 2, 3, and 4 indicate that <10%, 10–49%, 50–90%, and >90%, respectively, of the stomach mucosal area was affected.

Mucosa cell isolation and subcutaneous implantation to test transformation status
Stomachs from CTLA4KD mice and controls were dissected. The mucosa was excised and cut into small pieces. Tissues were treated with EDTA dissociation and collagenase digestion according to a procedure described before (Lui et al., 2015). The mucosal pieces were incubated in a solution con-

sisting of 10% FBS, 1× HBSS, 5 mM EDTA, and 15 mM Hepes and incubated at 37°C for 15 min on a horizontal shaker set to 250 RPM. Two rounds of dissociations were performed with the tissue. For each round, the dissociated cells were collected and filtered through an 80-μm filter. The filtrate was washed twice with 2% FBS and PBS and set on ice. The nondissociated tissue was thoroughly washed free of EDTA using 2% FBS and PBS. For collagenase digestion, the nondissociated tissue was resuspended in a digestion buffer consisting of type IV collagenase (100 U/ml; Sigma), and incubated at 37°C for 1 h on a horizontal shaker set at 250 RPM. The digested tissue was washed with 2% FBS and PBS and passed through an 80-μm filter. The filtrate was collected and pooled with the earlier isolations. This procedure was used for isolation of immune cells as well as mucosal cells. To test tumorigenic potential of the mucosal cells, 700,000 to 1,000,000 live cells were injected subcutaneously into 3- to 4-d-old CB6F1 pups. The CB6F1 recipients were generated by crossing mice on the BALB/c and B6 genetic background and were used to avoid allorejection of donor cells, which were from mice on the CB6F1 genetic background. The recipient mice were used starting at three-to-four days of age for the experiments to be completed before the weaning age or as early as possible, to reduce the duration and cost of the experiments. The mucosal cells from normal donor mice on the CB6F1 genetic background never grew in the recipients in those conditions. The pups were assessed for tissue growth at the injection site. The diameters of tumors were measured in millimeters. The tumors were preserved in 10% formalin and embedded in paraffin. Paraffin-embedded samples were sectioned and stained with H&E.

Quantification of gastric normal flora bacteria by quantitative PCR for *Helicobacter* or total bacterial loads.
The SPEM pathology caused by CTLA4 modulation is similar to that in B6 mice infected with *Helicobacter felis*, which prompted us to examine potential overgrowth of normal flora *Helicobacter*. As in many other facilities (Bohr et al., 2006), our SPF facility does not exclude *Helicobacter* species that are not considered pathogens. To investigate whether the metaplasia in CTLA4KD mice was caused by undetected normal flora *Helicobacter* overgrowth or undetected infection of pathogenic *Helicobacter*, we purified DNA from stomach samples and conducted a group-specific PCR assay for the *16S rRNA* gene of all known *Helicobacter* species (Bohr et al., 2006), or for all bacteria. SYBR green quantitative PCR was conducted with primers specific to the *16S rRNA* gene of all *Helicobacter* species, all bacterial species, or the eukaryotic gene β-casein. The relative levels of *16S rRNA* gene were normalized with the level of β-casein DNA in each sample.

Quantitative RT-PCR
The stomach sample was cut along the greater curvature and was flattened. The exposed luminal side was washed with sterile PBS. The clean stomach samples were transferred

to a disposable grinder unit, with mucosal surface remaining exposed. Trizol reagent (Thermo Fisher Scientific) was added immediately to the mucosal surface to preserve the RNA quality. A grinder plunger was then inserted into the tube with tissue samples and Trizol. The rough surface of the plunger was used to grind the mucosal tissues directly into the Trizol solution using gentle friction until the mucosal layer was visibly removed. This method was chosen for its consistency with animals at different ages and better quality of RNA preservation, especially when experimenting with very young animals, because technically, it was difficult to avoid contamination when dissecting the mucosa layer from the stomach samples of very young animals using instruments.

Quantitative RT-PCR array profiling for 84 oncogenes or tumor suppressor or related genes was done using a commercial kit (RT^2 Profiler PCR Array Mouse Oncogenes & Tumor Suppressor Genes; Qiagen), according to the manufacturer's protocol of assay and data analysis. The mRNA expression of some individual genes associated with stomach cancer specifically or cancer development in general, cell cycle control, cytokine receptors, or epigenetic regulation were also tested by quantitative RT-PCR. Relative units of mRNA levels (mean ± SEM) were calculated against HPRT or β-actin as the housekeeping gene.

Flow cytometry
Flow cytometry analyses were conducted with a standard procedure. The cells were stained with fluorescent antibody conjugates to determine cell phenotype. Intracellular cytokine staining was done with a standard procedure. The following antibody conjugates were used: PETR anti-CD8; eFluor450-conjugated anti-CD44; APC–eFluor780–conjugated anti-CD62L; PE-Cy7 and APC-eFluor780–conjugated anti-CD4; and PerCP-Cy5.5 conjugated anti-CD25 (Thermo Fisher Scientific). Intracellular cytokine staining was done with procedures described before (Devarajan et al., 2014; Pua et al., 2016). Cells were stimulated for 6 h in phorbol dibutyrate and ionomycin (Sigma), with brefeldin A (Thermo Fisher Scientific) added 4 h after the beginning of stimulation. Cells were stained for surface makers, and then fixed for 8 min in 4% paraformaldehyde. Cells were permeabilized in 0.5% saponin and blocked for 5 min at room temperature, followed up by addition of both PE-Cy7 or eFluor450–conjugated anti–IL-17A and PE-Cy7–conjugated anti–IFN-γ (BioLegend), APC-conjugated anti–IL-4, and PE-conjugated anti–IL-13 (Thermo Fisher Scientific) for 20 min at 4°C. Staining of c-Myc was done by fixation and permeabilization of the gastric tumor cells or normal gastric mucosal cells with fixation and permeabilization buffers (Thermo Fisher Scientific) followed by intracellular staining with Alexa Fluor 647–labeled anti–human c-MYC mAbs (clone 9E10; Thermo Fisher Scientific), which cross-reacts with mouse c-Myc, or Alexa Fluor 647–labeled IgG1 isotype control (BioLegend). Cells were analyzed with flow cytometers (LSR–II and Fortessa; Becton Dickinson) or CytoFLEX (Beckman Coulter).

Quantification of 5hmC in DNA and immunofluorescence staining for 5hmC in cell nuclei of tissue sections
DNA was purified from gastric mucosal tissue samples and analyzed via dot-blot as described in previous studies (Lian et al., 2012; Minor et al., 2013), with specific antibodies for 5hmC, and counterstained with methylene blue to normalize for total quantity.

Human GA samples were obtained from the Tissue Bank Core of the Sylvester Cancer Center at the University of Miami. For three of the samples, normal stomach mucosal tissue from the same patient was also obtained as matched controls. The tissues were embedded in OCT compound, and cryosections of the tumors and normal tissues at 7 μM thickness were prepared. The tissue sections were fixed with paraformaldehyde and stained with specific antibodies against 5hmC, as described in previous studies (Lian et al., 2012; Minor et al., 2013). In brief, cryosections were fixed in 4% paraformaldehyde for 15 min. After three washes with PBS, slides were treated with prewarmed 1 N HCl for 30 min at 37°C. Sections were then blocked with 3% normal donkey serum/0.4% Triton X-100 in PBS for 1 h at room temperature. Rabbit anti-5hmC antibody (Active Motif) was then added, incubated for overnight at 4°C, and followed with Cy3-conjugated donkey anti–rabbit antibody (Jackson ImmunoResearch Laboratories) in 2% normal donkey serum/0.1% Triton X-100 in PBS for 45 min at room temperature. After three washes in PBS, the slides were counterstained with DAPI mounting medium and imaged with a Leica inverted TCS SP-5 broadband confocal microscope (Leica 40×/1.25-0.75NA HCX PL APO oil-immersion lens). Images were then linearly contrasted and noise was removed using ImageJ software.

Statistics
Student's t tests or Mann–Whitney tests were used for single comparisons, and ANOVA was performed for multiple group analyses. For nonparametric multiple group analyses, Kruskal–Wallis analyses were performed with false discovery rate adjustment. The χ^2 test was used to assess incidence of inflammation and tumorigenesis (*, $P < 0.05$; **, $P < 0.01$; ***, $P < 0.001$; ns, not statistically significant).

Online supplemental material
Fig. S1 shows the characteristic SPEM pathology in the CTLA4KD models, which varies in extent on different genetic backgrounds. Fig. S2 presents evidence for malignant transformation of the gastric mucosal cells of aging CTLA4KD mice. Fig. S3 shows mRNA expression profiles in gastric mucosae of CTLA4KD mice for some genes associated with stomach cancer as well as cancer development in general. Fig. S4 shows the dysregulation of both type 1 and type 2 cytokine responses in CTLA4KD mice in the absence of detectable infection by pathogenic *Helicobacter*. Fig. S5 presents evidence of type 2 cytokine–driven signaling and epigenetic alteration in the gastric mucosal cells.

REFERENCES

Anderson, W.F., M.C. Camargo, J.F. Fraumeni Jr., P. Correa, P.S. Rosenberg, and C.S. Rabkin. 2010. Age-specific trends in incidence of noncardia gastric cancer in US adults. *JAMA.* 303:1723–1728. https://doi.org/10.1001/jama.2010.496

Anjos, S., A. Nguyen, H. Ounissi-Benkalha, M.C. Tessier, and C. Polychronakos. 2002. A common autoimmunity predisposing signal peptide variant of the cytotoxic T-lymphocyte antigen 4 results in inefficient glycosylation of the susceptibility allele. *J. Biol. Chem.* 277:46478–46486. https://doi.org/10.1074/jbc.M206894200

Ansel, K.M., I. Djuretic, B. Tanasa, and A. Rao. 2006. Regulation of Th2 differentiation and Il4 locus accessibility. *Annu. Rev. Immunol.* 24:607–656. https://doi.org/10.1146/annurev.immunol.23.021704.115821

Beck, K.E., J.A. Blansfield, K.Q. Tran, A.L. Feldman, M.S. Hughes, R.E. Royal, U.S. Kammula, S.L. Topalian, R.M. Sherry, D. Kleiner, et al. 2006. Enterocolitis in patients with cancer after antibody blockade of cytotoxic T-lymphocyte-associated antigen 4. *J. Clin. Oncol.* 24:2283–2289. https://doi.org/10.1200/JCO.2005.04.5716

Bohr, U.R., M. Selgrad, C. Ochmann, S. Backert, W. König, A. Fenske, T. Wex, and P. Malfertheiner. 2006. Prevalence and spread of enterohepatic Helicobacter species in mice reared in a specific-pathogen-free animal facility. *J. Clin. Microbiol.* 44:738–742. https://doi.org/10.1128/JCM.44.3.738-742.2006

Bratanič, N., J. Kovač, K. Pohar, K. Trebušak Podkrajšek, A. Ihan, T. Battelino, and M. Avbelj Stefanija. 2017. Multifocal gastric adenocarcinoma in a patient with LRBA deficiency. *Orphanet J. Rare Dis.* 12:131. https://doi.org/10.1186/s13023-017-0682-5

Bronte, V., P. Serafini, C. De Santo, I. Marigo, V. Tosello, A. Mazzoni, D.M. Segal, C. Staib, M. Lowel, G. Sutter, et al. 2003. IL-4-induced arginase 1 suppresses alloreactive T cells in tumor-bearing mice. *J. Immunol.* 170:270–278. https://doi.org/10.4049/jimmunol.170.1.270

Chambers, C.A., T.J. Sullivan, and J.P. Allison. 1997. Lymphoproliferation in CTLA-4-deficient mice is mediated by costimulation-dependent activation of CD4+ T cells. *Immunity.* 7:885–895. https://doi.org/10.1016/S1074-7613(00)80406-9

Chambers, C.A., M.S. Kuhns, J.G. Egen, and J.P. Allison. 2001. CTLA-4-mediated inhibition in regulation of T cell responses: mechanisms and manipulation in tumor immunotherapy. *Annu. Rev. Immunol.* 19:565–594. https://doi.org/10.1146/annurev.immunol.19.1.565

Chen, Z., J. Stockton, D. Mathis, and C. Benoist. 2006. Modeling CTLA4-linked autoimmunity with RNA interference in mice. *Proc. Natl. Acad. Sci. USA.* 103:16400–16405. https://doi.org/10.1073/pnas.0607854103

Correa, P. 1988. A human model of gastric carcinogenesis. *Cancer Res.* 48:3554–3560.

DeNardo, D.G., J.B. Barreto, P. Andreu, L. Vasquez, D. Tawfik, N. Kolhatkar, and L.M. Coussens. 2009. CD4(+) T cells regulate pulmonary metastasis of mammary carcinomas by enhancing protumor properties of macrophages. *Cancer Cell.* 16:91–102. https://doi.org/10.1016/j.ccr.2009.06.018

Devarajan, P., J. Miska, J.B. Lui, D. Swieboda, and Z. Chen. 2014. Opposing effects of CTLA4 insufficiency on regulatory versus conventional T cells in autoimmunity converge on effector memory in target tissue. *J. Immunol.* 193:4368–4380. https://doi.org/10.4049/jimmunol.1400876

Essner, R., Y. Huynh, T. Nguyen, M. Rose, M. Kojima, and D.S. Hoon. 2001. Functional interleukin-4 receptor and interleukin-2 receptor common gamma chain in human gastric carcinoma: a possible mechanism for cytokine-based therapy. *J. Gastrointest. Surg.* 5:81–90. https://doi.org/10.1016/S1091-255X(01)80017-2

Fox, J.G., and T.C. Wang. 2007. Inflammation, atrophy, and gastric cancer. *J. Clin. Invest.* 117:60–69. https://doi.org/10.1172/JCI30111

Gabrilovich, D.I., and S. Nagaraj. 2009. Myeloid-derived suppressor cells as regulators of the immune system. *Nat. Rev. Immunol.* 9:162–174. https://doi.org/10.1038/nri2506

Gandhi, N.A., B.L. Bennett, N.M. Graham, G. Pirozzi, N. Stahl, and G.D. Yancopoulos. 2016. Targeting key proximal drivers of type 2 inflammation in disease. *Nat. Rev. Drug Discov.* 15:35–50. https://doi.org/10.1038/nrd4624

Gause, W.C., T.A. Wynn, and J.E. Allen. 2013. Type 2 immunity and wound healing: evolutionary refinement of adaptive immunity by helminths. *Nat. Rev. Immunol.* 13:607–614. https://doi.org/10.1038/nri3476

Gocheva, V., H.W. Wang, B.B. Gadea, T. Shree, K.E. Hunter, A.L. Garfall, T. Berman, and J.A. Joyce. 2010. IL-4 induces cathepsin protease activity in tumor-associated macrophages to promote cancer growth and invasion. *Genes Dev.* 24:241–255. https://doi.org/10.1101/gad.1874010

Goldenring, J.R., K.T. Nam, T.C. Wang, J.C. Mills, and N.A. Wright. 2010. Spasmolytic polypeptide-expressing metaplasia and intestinal metaplasia: time for reevaluation of metaplasias and the origins of gastric cancer. *Gastroenterology.* 138:2207–2210: 2210.e1. https://doi.org/10.1053/j.gastro.2010.04.023

Hadinia, A., S.V. Hossieni, N. Erfani, M. Saberi-Firozi, M.J. Fattahi, and A. Ghaderi. 2007. CTLA-4 gene promoter and exon 1 polymorphisms in Iranian patients with gastric and colorectal cancers. *J. Gastroenterol. Hepatol.* 22:2283–2287. https://doi.org/10.1111/j.1440-1746.2007.04862.x

Hallett, M.A., K.T. Venmar, and B. Fingleton. 2012. Cytokine stimulation of epithelial cancer cells: the similar and divergent functions of IL-4 and IL-13. *Cancer Res.* 72:6338–6343. https://doi.org/10.1158/0008-5472.CAN-12-3544

Hayakawa, S., S. Okada, M. Tsumura, S. Sakata, Y. Ueno, K. Imai, T. Morio, O. Ohara, K. Chayama, and M. Kobayashi. 2016. A Patient with CTLA-4 Haploinsufficiency Presenting Gastric Cancer. *J. Clin. Immunol.* 36:28–32. https://doi.org/10.1007/s10875-015-0221-x

Hemminki, K., X. Liu, J. Ji, J. Sundquist, and K. Sundquist. 2012. Autoimmune disease and subsequent digestive tract cancer by histology. *Ann. Oncol.* 23:927–933. https://doi.org/10.1093/annonc/mdr333

Hodi, F.S., S.J. O'Day, D.F. McDermott, R.W. Weber, J.A. Sosman, J.B. Haanen, R. Gonzalez, C. Robert, D. Schadendorf, J.C. Hassel, et al. 2010. Improved survival with ipilimumab in patients with metastatic melanoma. *N. Engl. J. Med.* 363:711–723. https://doi.org/10.1056/NEJMoa1003466

Hou, R., B. Cao, Z. Chen, Y. Li, T. Ning, C. Li, C. Xu, and Z. Chen. 2010. Association of cytotoxic T lymphocyte-associated antigen-4 gene haplotype with the susceptibility to gastric cancer. *Mol. Biol. Rep.* 37:515–520. https://doi.org/10.1007/s11033-009-9705-1

Imrie, C., M. Rowland, B. Bourke, and B. Drumm. 2001. Is Helicobacter pylori infection in childhood a risk factor for gastric cancer? *Pediatrics.* 107:373–380. https://doi.org/10.1542/peds.107.2.373

Ise, W., M. Kohyama, K.M. Nutsch, H.M. Lee, A. Suri, E.R. Unanue, T.L. Murphy, and K.M. Murphy. 2010. CTLA-4 suppresses the pathogenicity of self antigen-specific T cells by cell-intrinsic and cell-extrinsic mechanisms. *Nat. Immunol.* 11:129–135. https://doi.org/10.1038/ni.1835

Jones, P.A. 2012. Functions of DNA methylation: islands, start sites, gene bodies and beyond. *Nat. Rev. Genet.* 13:484–492. https://doi.org/10.1038/nrg3230

June, C.H., J.T. Warshauer, and J.A. Bluestone. 2017. Is autoimmunity the Achilles' heel of cancer immunotherapy? *Nat. Med.* 23:540–547. https://doi.org/10.1038/nm.4321

Kuehn, H.S., W. Ouyang, B. Lo, E.K. Deenick, J.E. Niemela, D.T. Avery, J.N. Schickel, D.Q. Tran, J. Stoddard, Y. Zhang, et al. 2014. Immune dysregulation in human subjects with heterozygous germline mutations in CTLA4. *Science.* 345:1623–1627. https://doi.org/10.1126/science.1255904

Kushima, R., M. Vieth, F. Borchard, M. Stolte, K. Mukaisho, and T. Hattori. 2006. Gastric-type well-differentiated adenocarcinoma and pyloric gland adenoma of the stomach. *Gastric Cancer.* 9:177–184. https://doi.org/10.1007/s10120-006-0381-8

Lian, C.G., Y. Xu, C. Ceol, F. Wu, A. Larson, K. Dresser, W. Xu, L. Tan, Y. Hu, Q. Zhan, et al. 2012. Loss of 5-hydroxymethylcytosine is an epigenetic hallmark of melanoma. *Cell.* 150:1135–1146. https://doi.org/10.1016/j.cell.2012.07.033

Liang, H.E., R.L. Reinhardt, J.K. Bando, B.M. Sullivan, I.C. Ho, and R.M. Locksley. 2011. Divergent expression patterns of IL-4 and IL-13 define unique functions in allergic immunity. *Nat. Immunol.* 13:58–66. https://doi.org/10.1038/ni.2182

Ligers, A., N. Teleshova, T. Masterman, W.X. Huang, and J. Hillert. 2001. CTLA-4 gene expression is influenced by promoter and exon 1 polymorphisms. *Genes Immun.* 2:145–152. https://doi.org/10.1038/sj.gene.6363752

Lo, B., K. Zhang, W. Lu, L. Zheng, Q. Zhang, C. Kanellopoulou, Y. Zhang, Z. Liu, J.M. Fritz, R. Marsh, et al. 2015. AUTOIMMUNE DISEASE. Patients with LRBA deficiency show CTLA4 loss and immune dysregulation responsive to abatacept therapy. *Science.* 349:436–440. https://doi.org/10.1126/science.aaa1663

Loh, M., N. Liem, A. Vaithilingam, P.L. Lim, N.S. Sapari, E. Elahi, Z.Y. Mok, C.L. Cheng, B. Yan, B. Pang, et al. 2014. DNA methylation subgroups and the CpG island methylator phenotype in gastric cancer: a comprehensive profiling approach. *BMC Gastroenterol.* 14:55. https://doi.org/10.1186/1471-230X-14-55

Lozano, R., M. Naghavi, K. Foreman, S. Lim, K. Shibuya, V. Aboyans, J. Abraham, T. Adair, R. Aggarwal, S.Y. Ahn, et al. 2012. Global and regional mortality from 235 causes of death for 20 age groups in 1990 and 2010: a systematic analysis for the Global Burden of Disease Study 2010. *Lancet.* 380:2095–2128. https://doi.org/10.1016/S0140-6736(12)61728-0

Lui, J.B., P. Devarajan, S.A. Teplicki, and Z. Chen. 2015. Cross-differentiation from the CD8 lineage to CD4 T cells in the gut-associated microenvironment with a nonessential role of microbiota. *Cell Reports.* 10:574–585. https://doi.org/10.1016/j.celrep.2014.12.053

Maehara, Y., H. Anai, H. Kusumoto, and K. Sugimachi. 1987. Poorly differentiated human gastric carcinoma is more sensitive to antitumor drugs than is well differentiated carcinoma. *Eur. J. Surg. Oncol.* 13:203–206.

Miller, R.A., G. Buehner, Y. Chang, J.M. Harper, R. Sigler, and M. Smith-Wheelock. 2005. Methionine-deficient diet extends mouse lifespan, slows immune and lens aging, alters glucose, T4, IGF-I and insulin levels, and increases hepatocyte MIF levels and stress resistance. *Aging Cell.* 4:119–125. https://doi.org/10.1111/j.1474-9726.2005.00152.x

Minor, E.A., B.L. Court, J.I. Young, and G. Wang. 2013. Ascorbate induces ten-eleven translocation (Tet) methylcytosine dioxygenase-mediated generation of 5-hydroxymethylcytosine. *J. Biol. Chem.* 288:13669–13674. https://doi.org/10.1074/jbc.C113.464800

Miska, J., E. Bas, P. Devarajan, and Z. Chen. 2012. Autoimmunity-mediated antitumor immunity: tumor as an immunoprivileged self. *Eur. J. Immunol.* 42:2584–2596. https://doi.org/10.1002/eji.201242590

Miska, J., M.H. Abdulreda, P. Devarajan, J.B. Lui, J. Suzuki, A. Pileggi, P.O. Berggren, and Z. Chen. 2014. Real-time immune cell interactions in target tissue during autoimmune-induced damage and graft tolerance. *J. Exp. Med.* 211:441–456. https://doi.org/10.1084/jem.20130785

Morisaki, T., A. Uchiyama, D. Yuzuki, R. Essner, D.L. Morton, and D.S. Hoon. 1994. Interleukin 4 regulates G1 cell cycle progression in gastric carcinoma cells. *Cancer Res.* 54:1113–1118.

Nam, K.T., H.J. Lee, J.F. Sousa, V.G. Weis, R.L. O'Neal, P.E. Finke, J. Romero-Gallo, G. Shi, J.C. Mills, R.M. Peek Jr., et al. 2010. Mature chief cells are cryptic progenitors for metaplasia in the stomach. *Gastroenterology.* 139:2028–2037. https://doi.org/10.1053/j.gastro.2010.09.005

Nguyen, T.L., S.S. Khurana, C.J. Bellone, B.J. Capoccia, J.E. Sagartz, R.A. Kesman Jr., J.C. Mills, and R.J. DiPaolo. 2013. Autoimmune gastritis mediated by CD4+ T cells promotes the development of gastric cancer. *Cancer Res.* 73:2117–2126. https://doi.org/10.1158/0008-5472.CAN-12-3957

Noben-Trauth, N., L.D. Shultz, F. Brombacher, J.F. Urban Jr., H. Gu, and W.E. Paul. 1997. An interleukin 4 (IL-4)-independent pathway for CD4+ T cell IL-4 production is revealed in IL-4 receptor-deficient mice. *Proc. Natl. Acad. Sci. USA.* 94:10838–10843. https://doi.org/10.1073/pnas.94.20.10838

Oguma, K., H. Oshima, M. Aoki, R. Uchio, K. Naka, S. Nakamura, A. Hirao, H. Saya, M.M. Taketo, and M. Oshima. 2008. Activated macrophages promote Wnt signalling through tumour necrosis factor-alpha in gastric tumour cells. *EMBO J.* 27:1671–1681. https://doi.org/10.1038/emboj.2008.105

Phan, G.Q., J.C. Yang, R.M. Sherry, P. Hwu, S.L. Topalian, D.J. Schwartzentruber, N.P. Restifo, L.R. Haworth, C.A. Seipp, L.J. Freezer, et al. 2003. Cancer regression and autoimmunity induced by cytotoxic T lymphocyte-associated antigen 4 blockade in patients with metastatic melanoma. *Proc. Natl. Acad. Sci. USA.* 100:8372–8377. https://doi.org/10.1073/pnas.1533209100

Pua, H.H., D.F. Steiner, S. Patel, J.R. Gonzalez, J.F. Ortiz-Carpena, R. Kageyama, N.T. Chiou, A. Gallman, D. de Kouchkovsky, L.T. Jeker, et al. 2016. MicroRNAs 24 and 27 Suppress Allergic Inflammation and Target a Network of Regulators of T Helper 2 Cell-Associated Cytokine Production. *Immunity.* 44:821–832. https://doi.org/10.1016/j.immuni.2016.01.003

Ren, Z., G. Pang, R. Clancy, L.C. Li, C.S. Lee, R. Batey, T. Borody, and M. Dunkley. 2001. Shift of the gastric T-cell response in gastric carcinoma. *J. Gastroenterol. Hepatol.* 16:142–148. https://doi.org/10.1046/j.1440-1746.2001.02385.x

Sapari, N.S., M. Loh, A. Vaithilingam, and R. Soong. 2012. Clinical potential of DNA methylation in gastric cancer: a meta-analysis. *PLoS One.* 7:e36275. https://doi.org/10.1371/journal.pone.0036275

Schubert, D., C. Bode, R. Kenefeck, T.Z. Hou, J.B. Wing, A. Kennedy, A. Bulashevska, B.S. Petersen, A.A. Schäffer, B.A. Grüning, et al. 2014. Autosomal dominant immune dysregulation syndrome in humans with CTLA4 mutations. *Nat. Med.* 20:1410–1416. https://doi.org/10.1038/nm.3746

Sharon, E. 2017. Can an Immune Checkpoint Inhibitor (Sometimes) Make Things Worse? *Clin. Cancer Res.* 23:1879–1881. https://doi.org/10.1158/1078-0432.CCR-16-2926

Siosaki, M.D., and A.T. Souza. 2013. Images in clinical medicine. Virchow's node. *N. Engl. J. Med.* 368:e7. https://doi.org/10.1056/NEJMicm1204740

Soutto, M., A. Belkhiri, M.B. Piazuelo, B.G. Schneider, D. Peng, A. Jiang, M.K. Washington, Y. Kokoye, S.E. Crowe, A. Zaika, et al. 2011. Loss of TFF1 is associated with activation of NF-κB–mediated inflammation and gastric neoplasia in mice and humans. *J. Clin. Invest*. 121:1753–1767. https://doi.org/10.1172/JCI43922

Tivol, E.A., F. Borriello, A.N. Schweitzer, W.P. Lynch, J.A. Bluestone, and A.H. Sharpe. 1995. Loss of CTLA-4 leads to massive lymphoproliferation and fatal multiorgan tissue destruction, revealing a critical negative regulatory role of CTLA-4. *Immunity*. 3:541–547. https://doi.org/10.1016/1074-7613(95)90125-6

Toh, B.H., I.R. van Driel, and P.A. Gleeson. 1997. Pernicious anemia. *N. Engl. J. Med*. 337:1441–1448. https://doi.org/10.1056/NEJM199711133372007

Toomer, K.H., and Z. Chen. 2014. Autoimmunity as a double agent in tumor killing and cancer promotion. *Front. Immunol*. 5:116. https://doi.org/10.3389/fimmu.2014.00116

Tu, S., G. Bhagat, G. Cui, S. Takaishi, E.A. Kurt-Jones, B. Rickman, K.S. Betz, M. Penz-Oesterreicher, O. Bjorkdahl, J.G. Fox, and T.C. Wang. 2008. Overexpression of interleukin-1beta induces gastric inflammation and cancer and mobilizes myeloid-derived suppressor cells in mice. *Cancer Cell*. 14:408–419. https://doi.org/10.1016/j.ccr.2008.10.011

Volkers, N. 1999. Do autoimmune diseases raise the risk of cancer? *J. Natl. Cancer Inst*. 91:1992–1993. https://doi.org/10.1093/jnci/91.23.1992

Wang, X.B., X. Zhao, R. Giscombe, and A.K. Lefvert. 2002. A CTLA-4 gene polymorphism at position –318 in the promoter region affects the expression of protein. *Genes Immun*. 3:233–234. https://doi.org/10.1038/sj.gene.6363869

Waterhouse, P., J.M. Penninger, E. Timms, A. Wakeham, A. Shahinian, K.P. Lee, C.B. Thompson, H. Griesser, and T.W. Mak. 1995. Lymphoproliferative disorders with early lethality in mice deficient in Ctla-4. *Science*. 270:985–988. https://doi.org/10.1126/science.270.5238.985

Wing, K., Y. Onishi, P. Prieto-Martin, T. Yamaguchi, M. Miyara, Z. Fehervari, T. Nomura, and S. Sakaguchi. 2008. CTLA-4 control over Foxp3+ regulatory T cell function. *Science*. 322:271–275. https://doi.org/10.1126/science.1160062

Wroblewski, L.E., R.M. Peek Jr., and K.T. Wilson. 2010. Helicobacter pylori and gastric cancer: factors that modulate disease risk. *Clin. Microbiol. Rev*. 23:713–739. https://doi.org/10.1128/CMR.00011-10

Wynn, T.A. 2015. Type 2 cytokines: mechanisms and therapeutic strategies. *Nat. Rev. Immunol*. 15:271–282. https://doi.org/10.1038/nri3831

Yao, T., T. Utsunomiya, M. Oya, K. Nishiyama, and M. Tsuneyoshi. 2006. Extremely well-differentiated adenocarcinoma of the stomach: clinicopathological and immunohistochemical features. *World J. Gastroenterol*. 12:2510–2516. https://doi.org/10.3748/wjg.v12.i16.2510

Zeissig, S., B.S. Petersen, M. Tomczak, E. Melum, E. Huc-Claustre, S.K. Dougan, J.K. Laerdahl, B. Stade, M. Forster, S. Schreiber, et al. 2015. Early-onset Crohn's disease and autoimmunity associated with a variant in CTLA-4. *Gut*. 64:1889–1897. https://doi.org/10.1136/gutjnl-2014-308541